International Journal of Chemical, Materials and Biomolecular Sciences
ISSN: 2415-6620
Vol:7, No:6, 2013

Numerical Investigation of Nozzle Shape Effect on Shock Wave in Natural Gas Processing

Esam I. Jassim and Mohamed M. Awad

***Abstract*—**Natural gas flow contains undesirable solid particles, liquid condensation, and/or oil droplets and requires reliable removing equipment to perform filtration. Recent natural gas processing applications are demanded compactness and reliability of process equipment. Since conventional means are sophisticated in design, poor in efficiency, and continue lacking robust, a supersonic nozzle has been introduced as an alternative means to meet such demands.

A 3-D Convergent-Divergent Nozzle is simulated using commercial Code for pressure ratio (NPR) varies from 1.2 to 2. Six different shapes of nozzle are numerically examined to illustrate the position of shock-wave as such spot could be considered as a benchmark of particle separation. Rectangle, triangle, circular, elliptical, pentagon, and hexagon nozzles are simulated using Fluent Code with all have same cross-sectional area.

The simple one-dimensional inviscid theory does not describe the actual features of fluid flow precisely as it ignores the impact of nozzle configuration on the flow properties. CFD Simulation results, however, show that nozzle geometry influences the flow structures including location of shock wave.

The CFD analysis predicts shock appearance when p_{01}/p_a>1.2 for almost all geometry and locates at the lower area ratio (A_e/A_t). Simulation results showed that shock wave in Elliptical nozzle has the farthest distance from the throat among the others at relatively small NPR. As NPR increases, hexagon would be the farthest. The numerical result is compared with available experimental data and has shown good agreement in terms of shock location and flow structure.

***Keywords*—**CFD, Particle Separation, Shock wave, Supersonic Nozzle.

I. Introduction

IN gas processing industry, gas-expansion equipment is employed for obtaining low temperatures. As a result, natural gas flow could contain solid particles, liquid condensation, and/or oil droplets. Existing such undesirable phases in any natural gas pipeline might cause several problems in equipment and instrumentations. For instant, solid particles could deposit on the pipe wall leading to partially blockage the flow. The consequences could be worse as the accumulation grows up resulting in losing in flow pressure and reduction in transmission efficiency.

Particle layers propagation tend to gradually form a plug that separates the pipe into two pressure sections: a high pressure section between the high pressure gas source and the plug and a second section at low pressure between the plug and the gas recovery division. In the upstream section, a pipe blast can occur due to pressure rise. The plug can also behave as a projectile that destroys the pipe when the pressure difference between the upstream and downstream sections increases.

The deposition of particles inside gas pipelines is extremely undesired due to its environmentally and economically dangerous impact. The problems come up when the solid material clogs the fluid stream, even increasing pressure drop and causing pipe leaks or explosion.

Also, a pipeline blow-out endangers human life as such accidents have resulted in human deaths in the past. In one incident, an explosion caused a large piece of pipe to strike the foreman, killing him [1]. Lysne [2] listed three incidents in which projectiles erupted from pipelines at elbows had caused loss of three lives and over $7 million (US) in capital costs. Another example is the Piper Alpha disaster in the North Sea of July 6th, 1988 which clearly demonstrated the catastrophic consequence of this type of failure where 165 of the 226 on board died. Further, the energy released during this tragedy was estimated to be equal to 20% of the UK energy consumption for that period [1].

The blockage incident due to deposition in natural gas pipeline that occurred on the Gas Export Pipeline (GEP) of the Matterhorn platform in 2007 had required three days for resuming [3]. During the remediation process, about 2400 bbl of condensate and 5 MMscf of gas were blown out. Statistical data showed that annually an operating expense greater than $500 million is allocated for particle deposition prevention [4], almost half of which spent for inhibitors [5]. Insulation of subsea Natural gas pipelines costs up to $1,000,000 per mile to alleviate second phase formation [5].

Although filtration process captures large particles (mainly >15μm), smaller size particles will escape the process and need to be effectively removed. Besides, the collision of the particles with the fibers of filtration media reduces the kinetic energy of the particles imported by the gas stream, eventuating adhering on the pipe wall. Such problems, among many others, turned researcher's attentions to invent other methods of gas purification. However, coming up with a robust design that have capability to perform the task with minor problems is a challenge. Since the common design challenges in all natural gas-expansion applications are the compactness and reliability of process equipment, supersonic nozzles has been introduced as an alternative device to meet such demands.

Recent research has introduced state of art technologies based on adiabatic cooling, the process of gas expansion in a supersonic nozzle employed for obtaining low temperatures. During the process, part of gas enthalpy transforms to kinetic

Esam Jassim is with the Prince Mohammed Bin Fahd University (phone: +9663-849-9314; fax: +9663-896-4566; e-mail: ejassim@ pmu.edu.sa).

energy on expenses of temperature. The gained kinetic energy can be reused to increase the pressure in the system of supersonic and subsonic diffusers. The nozzle working section liquefies target components and significantly decreases pressure and temperature at exit without utilizing external energy.

Solid Particles and condensed droplets are separated due to centrifugal forces that formed by swirling the gas ahead or at the outlet of the supersonic nozzle. The latter method has been used by Twister BV, Rijswijk, Netherlands [6], [7]. Installing a blade at the end of the nozzle in the supersonic flow zone immediately before the extraction device provides swirling to the gas passing through it. The Twister separator dehydrates gas and separates heavy hydrocarbons [8].

The former method, using a swirling device in the plenum chamber ahead of the nozzle, was independently proposed by a group of Russian specialists and developed with their participation by TransLang Technologies Ltd., Calgary. This method initiates gas swirling in the plenum chamber so that the tangential velocities, when combined with the centrifugal forces, separate any second phase particles formed in the supersonic nozzle and deliver them to a special extracting equipment. This approach minimizes total pressure losses in the shock waves and separates the flow deceleration zone behind the shock wave from the drop separation zone [8].

The compact design of supersonic nozzles is a major advantage over traditional means of natural gas treating technology. Comparison with other conventional devices such as Joul-Thompson valve and turboexpander has been experimentally studied. Measurements showed that significant privileges are manifested, in particular energy consumption and device compatibility. Moreover, the high speed of the gas prevents fouling or deposition of particles and the shock wave that would be generated will increase the vortex potential of the flow, assisting in capturing smaller particles and recovering the pressure of the flow [9].

Flow regime in Laval Nozzle of different geometry and sizes has been numerously investigated experimentally and computationally. Esam et al [10] have examined the impact of geometry on the shock position numerically. They claimed that variation of divergent part of the nozzle would significantly change the location of the shock wave.

The simplifying of complex flow in nozzle by assuming one-dimensional flow results in significant erroneous in predicting flow structure. In reality, viscous effects, boundary layer/shock interaction, and flow separation drastically alter the features of the flow.

Commercial software has been employed to investigate the discrepancy of simple one-dimensional theory with the numerical simulation outcome. Work of Khan et al. [11] on the 2D convergent-divergent nozzle has shown that the location of shock predicted by analytical theory drastically differs from computed simulation.

Raman et al. [12] presented their computational and experimental works on flow separation over wide range of NRP. Their results are used to further examine the impact of the separated flow.

In term of particle separation potential, Supersonic nozzle has been experimentally examined together with other conventional devices. The outcome proved that at same extraction level, plants used nozzle as a separation device consume 10-20% less compressor power than those used a Joule-Thomson valve or turboexpander [1]. This may return to the fact that acceleration gained by the particle passes through the shock is huge and could be even touch the order of 10^6 times gravity acceleration [10].

Mzad and Elguerri [13] have presented the impact of the nozzle geometry on the flow physical behavior along the CD nozzle. Two different lengths in the divergent portion were employed. The analytical interpretation of their work has been verified by flow visualization and pressure measurements. Their experimental results concluded that the performance of the flow in CD nozzle could not be described by simple 1-D assumption as the flow behavior is widely differed from theory prediction. The experimental measurements showed that extending the divergent part of nozzle requires higher NPR to form shock. Similar conclusion was proposed by Esam et al. [10], who conducted numerical study on 2-D CD nozzle with extended length.

So far, there is indispensable demand to identify optimal shape of supersonic nozzle that is capable to separate particles more efficiently.

The objective of the present work is to elucidate the impact of nozzle shape on the location of shock wave and flow behavior by employing CFD Fluent code. A Reynolds-avergedNavier-Stokes equation with k-ε equation turbulence is used to predict shock position in symmetric 3-D nozzle. The experimental results of Papamoschou and Zill [14] are utilized as benchmark for assessment.

II. Theory and Mathematical Modeling

The aim of this section is to brief the procedure of determination the streamwise location of shock wave with knowledge of nozzle geometry and NPR.

Conservation of energy equation for 1-D invisid flow is written as:

$$udu + \frac{dP}{\rho} = 0 \tag{1}$$

By ignoring the flow velocity at nozzle entrance, integration of (1) leads to evaluation of flow velocity at any location along the nozzle:

$$u = \sqrt{\frac{2\gamma}{(\gamma-1)}\frac{P_0}{\rho_0}\left[1-\left(\frac{P}{P_0}\right)^{\frac{\gamma-1}{\gamma}}\right]} \tag{2}$$

Introducing Mach number and rearrange for pressure ratio, (2) might take the following form:

$$\frac{P}{P_0} = \left[1+\frac{\gamma-1}{2}M^2\right]^{-\left(\frac{\gamma}{\gamma-1}\right)} \tag{3}$$

The relation between local Mach number and the area at that location is defined by:

$$\frac{A}{A^*}=\frac{1}{M}\left[\frac{2}{\gamma+1}\left(1+\frac{\gamma-1}{2}M^2\right)\right]^{\frac{\gamma+1}{2(\gamma-1)}} \tag{4}$$

where A^* stands for the throat area.

The product of (3) and (4) would be:

$$\left(\frac{A}{A^*}\right)\left(\frac{P}{P_0}\right)=\frac{1}{M}\left[1+\frac{\gamma-1}{2}M^2\right]^{-1/2}\left[\frac{2}{\gamma+1}\right]^{\frac{\gamma+1}{2(\gamma-1)}} \tag{5}$$

Applying (5) on Nozzle exit:

$$\left(\frac{A_e}{A^*}\right)\left(\frac{1}{NPR}\right)=\frac{1}{M_e}\left[1+\frac{\gamma-1}{2}M_e^2\right]^{-1/2}\left[\frac{2}{\gamma+1}\right]^{\frac{\gamma+1}{2(\gamma-1)}} \tag{6}$$

Equation (6) can be rewritten in quadratic form for M_e:

$$\left(\frac{\gamma-1}{2}\right)\times\left[M_e^2\right]^2+M_e^2-\frac{1}{C^2}=0 \tag{7}$$

where

$$C=\left(\frac{A_e}{A^*}\right)\left(\frac{1}{NPR}\right)\times\left[\frac{2}{\gamma+1}\right]^{-\left(\frac{\gamma+1}{2(\gamma-1)}\right)}$$

by solving the quadratic equation, knowing that Mach number must be positive, the flow exit Mach number is determined by:

$$M_e^2=\frac{1}{\gamma-1}\left[\sqrt{1+\frac{2(\gamma-1)}{C^2}}-1\right] \tag{8}$$

Equation (8) relates NPR, divergent portion geometry of the nozzle, and exit Mach number. As mentioned earlier in this section, the goal is to come up with a procedure that uses the right hand side of (8) to evaluate the shock location (A/A^*). Such expressions can be obtained as follows:

The total pressure ratio across the shock (P_{02}/P_{01}) could be written as:

$$\frac{P_{02}}{P_{01}}=\left(\frac{P_{02}}{P_e}\frac{P_e}{P_{01}}\right)=\left(\frac{P_{02}}{P_e}\frac{1}{NPR}\right) \tag{9}$$

For isentropic flow, the inlet and exit total pressures are equal to the shock upstream and downstream total pressures, respectively. By applying (3) at nozzle exit, (9) yields to:

$$\frac{P_{02}}{P_{01}}=\left(1+\frac{\gamma-1}{2}M_e^2\right)^{\frac{\gamma}{\gamma-1}}\frac{1}{NPR} \tag{10}$$

Once the total pressure ratio across the shock is determined, the upstream Mach number can be found by employing the shock wave relation, which takes the form:

$$\frac{P_{02}}{P_{01}}=\left[\frac{\frac{\gamma+1}{2}M_1^2}{1+\frac{\gamma-1}{2}M_1^2}\right]^{\frac{\gamma}{\gamma-1}}\left[\frac{2\gamma}{\gamma+1}M_1^2-\frac{\gamma-1}{\gamma+1}\right]^{\frac{1}{\gamma-1}} \tag{11}$$

Finally, the area at which the shock occurs is determined from (4):

$$\frac{A}{A^*}=\frac{1}{M_1}\left[\frac{2}{\gamma+1}\left(1+\frac{\gamma-1}{2}M_1^2\right)\right]^{\frac{\gamma+1}{2(\gamma-1)}} \tag{12}$$

Hence, the procedure of determination the shock location by knowing NPR and exit to throat area ratio can be summarized as follows:

1. As NPR and A_e/A^* known, Mach number at exit (M_e) is evaluated using (8).
2. From outlet Mach number and NPR, total pressure ratio across the shock is determined from (10).
3. Shock wave relation, (11), is employed to find shock upstream Mach number (M_1).
4. Equation (12) is used for determining shock wave area.

The presence of the shock wave changes all flow conditions across it except the stagnation temperature (or, more precisely, the stagnation enthalpy) since across the shock the flow is adiabatic. The extent of the influence of the shock on the flow conditions depends upon the Mach number of the flow going into the shock.

For thermally and calorically perfect gases, the ratio of the static pressures across the shock (p_2/p_1) as a function of Mach number ahead of the shock (M_1) and the relation between Mach numbers before and after shock wave are respectively given by:

$$\frac{p_2}{p_1}=\frac{2\gamma M_1^2-(\gamma-1)}{\gamma+1} \tag{13}$$

$$M_2=\left[\frac{1+[(\gamma-1)/2]M_1^2}{\gamma M_1^2-(\gamma-1)/2}\right]^{1/2} \tag{14}$$

Comparsion of those relations with the 3-D CFD results is conducted in this study to examine the range of errounous that the 1-D assumption would be.

III. Numerical Simulation

The finite volume solver, FLUENT 6.3.26, is used to obtain the numerical solution of the three-dimensional compressible Navier–Stokes (RANS) equations in connection with (k-ε)turbulence model equation.

The discretized equations, along with the initial condition and boundary conditions, were solved using the segregated solution method, in which the conservation of mass and momentum were solved sequentially and a pressure correction equation (SIMPLE Scheme) was used to ensure the conservation of momentum and the conservation of mass (continuity equation).

IV. The Governing Equations

The governing equations consist of the continuity equation and the Reynolds-averaged governing equations for steady compressible turbulent flow coupled with the equation of state, p = qRT. The system of the governing equations can be described as follows:

The continuity equation:

$$\frac{\partial}{\partial x_i}(\rho u_i) = 0 \tag{15}$$

RANS equation:

$$\frac{\partial}{\partial x_j}(\rho u_i u_j) = -\frac{\partial p}{\partial x_i} + \frac{\partial}{\partial x_j}\left[\mu\left(\frac{\partial u_i}{\partial x_j} + \frac{\partial u_j}{\partial x_i} - \frac{2}{3}\delta_{ij}\frac{\partial u_l}{\partial x_l}\right)\right] + \frac{\partial}{\partial x_j}(-\rho\overline{u_i' u_j'}) \tag{16}$$

Energy equation:

$$\frac{\partial}{\partial t}(\rho E) + \frac{\partial}{\partial x_i}[u_i(\rho E + p)] = \frac{\partial}{\partial x_j}\left(\left(k + \frac{C_p \mu_t}{0.85}\right)\frac{\partial T}{\partial x_j} + u_i(-\rho\overline{u_i' u_j'})\right) \tag{17}$$

A. Turbulence Model

Although several turbulence models are available, most of these models are actually derived from standard (*k*-*ε*)model. However they are vary in complexity and robustness from two equation turbulence models to more elaborated turbulence model.

In the present work, the standard (*k*-*ε*)model is employed to predict the flow behavior in the considered physical domain.

B. Eddy Viscosity Models (EVM)

The apparent turbulent shearing stresses might be related to the rate of mean strain through an apparent scalar turbulent or ‘‘eddy’’ viscosity. For the general Reynolds stress tensor, the Boussinesq assumption gives:

$$-\rho\overline{u_i' u_j'} = \mu_t\left(\frac{\partial u_i}{\partial x_j} + \frac{\partial u_j}{\partial x_i}\right) - \frac{2}{3}\left(\rho k + \mu_t \frac{\partial u_k}{\partial x_k}\right)\delta_{ij} \tag{18}$$

where δ_{ij} is the Kronecker delta function ($\delta_{ij} = 1$ if i = j and $\delta_{ij} = 0$ if $i \neq j$), k is the turbulent kinetic energy and μ_t is the turbulent viscosity. In order to obtain the turbulent viscosity, other transport equations are needed. Theses equations differ from one model to another. The general transport equations for the adopted model are given below, while the different terms and coefficient of the turbulence models adopted are given in Table I.

The *k*-equation:

$$\frac{\partial}{\partial x_j}(\rho u_i k) = \frac{\partial}{\partial x_j}\left[\left(\mu + \frac{\mu_t}{\sigma_k}\right)\frac{\partial k}{\partial x_j}\right] + \rho(P_k^* - \beta_1\varepsilon - \beta_2 k\omega) \tag{19}$$

The *ε*-equation:

$$\frac{\partial}{\partial x_j}(\rho u_i \varepsilon) = \frac{\partial}{\partial x_j}\left[\left(\mu + \frac{\mu_t}{\sigma_\varepsilon}\right)\frac{\partial \varepsilon}{\partial x_j}\right] + \frac{\rho}{T}\left(C_{1\varepsilon}P_k - C_{2\varepsilon}\varepsilon + C_{3\varepsilon}\frac{P_k^2}{\varepsilon}\right) \tag{20}$$

TABLE I
Coefficients of Turbulent Models

STD *ε*-*K* MODEL	
β_1	1
β_2	0
β_3	0
σ_K	1
σ_E	1.3
σ_ω	0
P_k	$2\nu_t S_{ij} S_{ij}$
S_{ij}	$0.5(u_{i,xj}+u_{j,xi})$
P_k^*	P_k
$C_{1\varepsilon}$	1.4
$C_{2\varepsilon}$	1.92
$C_{3\varepsilon}$	0
T	k/ε
μ_t	$\rho C_\mu k^2/\varepsilon$
C_μ	0.09
L	0
F_2	0
D_1	0
γ_1	0
F_{SST}	0
F_1	0
D_2	0
D_3	0

V. Validation with Experiments

In order to validate the accuracy of the numerical simulation, comparison with the experimental data reported by Papamoschou and Zill [14] has been conducted. The geometry illustrated in Fig. 1 has the following dimensions at exit: height H =22.9mm, width *w* =63.5mm, and length *L* =117mm from throat to exit.

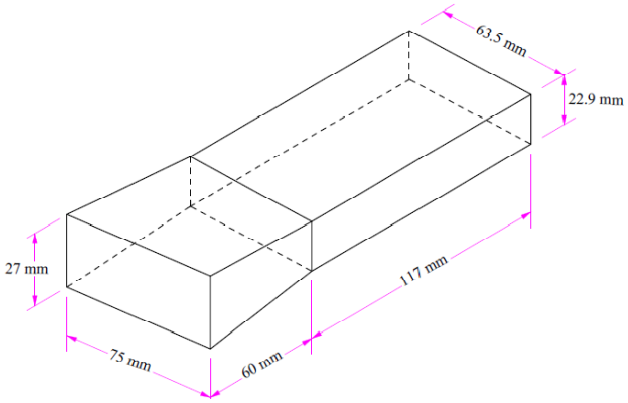

Fig. 1 Schematic of C-D Nozzle [13]

Our comparison for shock formation as NPR increases is presented for A_e/A_t = 1.4. The CFD analysis predicts shock appearance when p_{01}/p_a>1.2 and locates at the lower area ratio. The locations of the shock wave for various NPR predicted by CFD simulation along with the experimental measurements performed by [14] are depicted in Fig. 2. The 1-D analytical formulas are also employed and plotted in the figure to demonstrate the discrepancy of analytical approach with numerical and experimental outcomes. The normalized area of the shock position w.r.t. throat area (A/A_t) is plotted against the NPR. As illustrated in the figure, the prediction of shock wave location using 1-D approximation is widely far from CFD result and experimental measurement, particularly at high NPR. In return, 3-D numerical results are shown to be in good agreement with the experimental data.

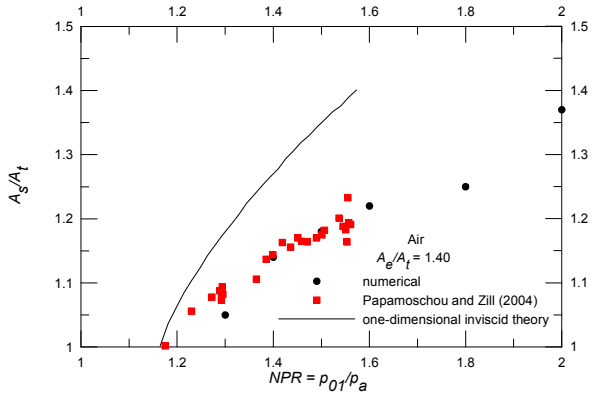

Fig. 2 Shockwave location predicted by CFD simulation vs. Experimental data performed by [14]

Contours of Mach number at centerline plane are plotted for different NPR. As observed in Fig. 3, for NPR = 1.2 the flow does not reach sonic value at throat. Hence, the C-D nozzle behaves as a subsonic flow. This significant conclusion controverts the results of 1-D equations, which predict shock existence at $A_s/A_t \approx 1.05$. As the NPR increases, the shock manifests near the throat and moves firmly toward the exit of the divergent part of the nozzle.

Fig. 4 depicts the impact of nozzle shape on shock location as a function of NPR. Although nozzle shape factor is not included in the governing equations that present the gas motion in the supersonic nozzle, CFD results confirm that a slight deviation in the shock location occurs when the geometry of the nozzle is changed.

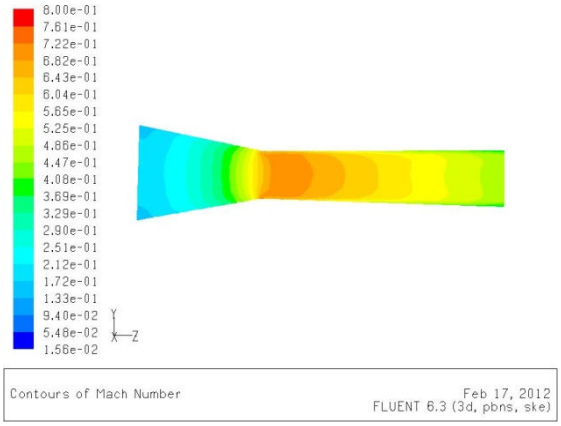

(a) NPR=1.2

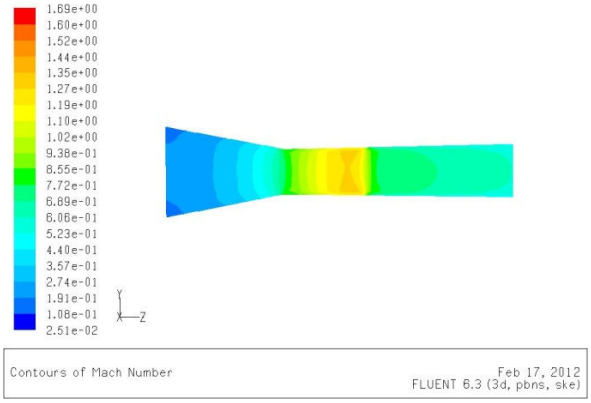

(b) NPR=1.4

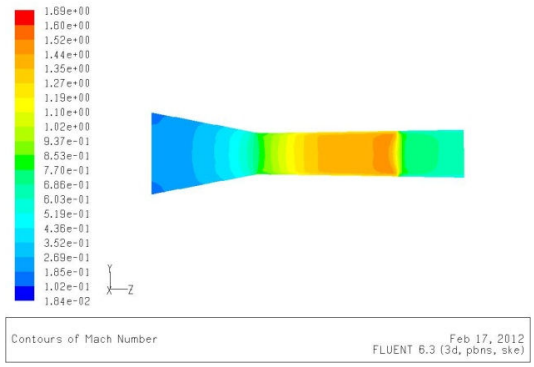

(c) NPR=1.6

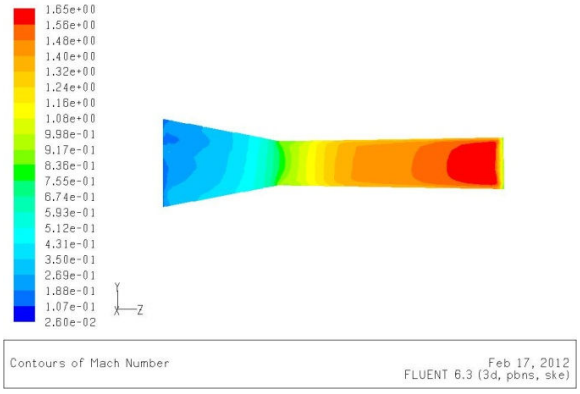

(d) NPR=2.0

Fig. 3 Contours of Mach number at Centre Plane

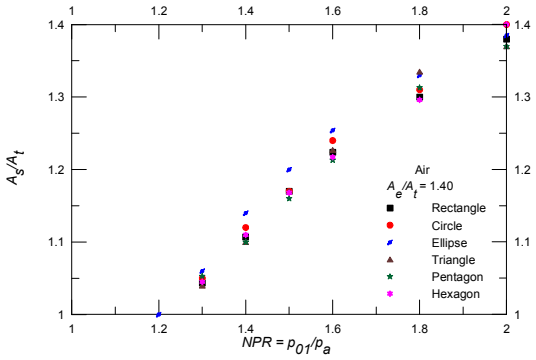

Fig. 4 Shockwave location predicted by CFD simulation for different circular and noncircular shapes

VI. Conclusion

Separation of undesirable particles from natural gas flow using supersonic nozzle is a promised technology that turns oil and gas firm's attention to enhance the already existing systems. Utilizing supersonic nozzle for this purpose has showed a positive impact on the separation technology due to simplicity in designing, cost effective in manufacturing, and feasibility in maintenance.

The research in this work focus mainly on employing CFD commercial software to study the influence of nozzle shape on the shockwave location since such location impacts the turbulence of the flow that eventually forces small particles to move toward the nozzle wall. Hence, improves the collection efficiency.

The numerical results show that nozzle shape is slightly changed with the shape of the nozzle. Elliptical Nozzle predicts shockwave a bit later than other shapes for specific NPR. However at high NPR hexagon nozzle is the one among the rest whose shock location becomes the farthest from the nozzle throat.

References

[1] www.experimentation-online.co.uk/article.php?id=1390

[2] Lysne D., "An Experimental Study of Hydrate Plug Dissociation by Pressure Reduction," Ph.D. Thesis, Norwegian Institute of Technology, University of Trondhiem, 1995

[3] Moussa Kane, Aditya Singh, and Ronny Hanssen, "Hydrates Blockage Experience in a Deep Water Subsea Dry Gas Pipeline: Lessons Learned", at the 2008 Offshore Technology Conference held in Houston, Texas, U.S.A., 5–8 May 2008.

[4] Lederhos J.P., Long J.P, Sum A., Christiansen R.L., Sloan E.D., "Effective Kinetic Inhibitors For Natural Gas Hydrates", Chemical Engineering Science, 51(8), 1221-1229, 1996.

[5] Sloan E.D, "Fundamental principles and applications of Natural Gas Hydrates", Nature Publication Group, 426, 353-359, Nov. 2003.

[6] Cottrll, A. "Technique puts gas treatment in a spin," Upstream, Mar. 19, 2004, p. 48.

[7] Okimoto, F., and Brouwer, J., "Supersonic gas condition," World Oil, August 2002.

[8] VadimAlfyorov; Lev Bagirov; Leonard Dmitriev; Vladimir Feygin; SalavatImaev; John R. Lacey, Supersonic nozzle efficiently separates natural gas components, Oil and Gas Journal, volume 103, issue 20, 2005.

[9] Jassim E., AbedinzadeganAbdi M., and Muzychka Y., "Computational Fluid Dynamics Study for Flow of Natural Gas through High Pressure Supersonic Nozzles: Part 1- Real Gas Effects and Shockwave", Journal of Petroleum Science and Technology, Vol. 26 issue 15, 1757-1772, 2008.

[10] Jassim E., AbedinzadeganAbdi M., and Muzychka Y., "Computational Fluid Dynamics Study for Flow of Natural Gas through High Pressure Supersonic Nozzles: Part 2- Nozzle Geometry and Vorticity", Journal of Petroleum Science and Technology, Vol. 26 issue (15), 1773-1785, 2008.

[11] A.A.Khan and T.R. Shembharkar: Viscous flow analysis in a convergent divergent Nozzle, Proc. Of the Int. Conf. on Aerospace Sci. and Technology, June 26-28 2008, Bangalore, India

[12] M.V.Raman, C.S. Kumar and S. Elangovan: An experimental and numerical investigation of supersonic contour nozzle flow separation, Proceeding in the Int. Conf. on Aerospace Sci. and Technology, June 26-28 2008, Bangalore, India.

[13] H. Mzad and M. Elguerri: Theoretical and experimental investigation of compressible flow through convergent-divergent nozzles, Advanced Materials Research,Vol 452-453 (2012),pp 1277-1285, Switzerland.

[14] D.Papamoschou, A.Zill and A.Johnson: Supersonic flow separation in Planar Nozzles, Shock waves, Vol. 19/3 (2008), pp. 171-183.